A quasiclassical trajectory study of the H+HCN→H_2+CN reaction dynamics

Diego Troya and Irene Baños
Departamento de Química, Universidad de La Rioja, C/ Madre de Dios 51, 26006 Logroño, Spain

Miguel González
Departament de Química Física i Centre de Recerca en Química Teòrica, Universitat de Barcelona, C/ Martí i Franquès 1, 08028 Barcelona, Spain

Guosheng Wu, Marc A. ter Horst, and George C. Schatz
Department of Chemistry, Northwestern University, 2145 Sheridan Rd, Evanston, IL 60208-3113

(Received 8 June 2000; accepted 18 July 2000)

We present a quasiclassical trajectory study of the title reaction using a potential energy surface that is derived from *ab initio* calculations, and which has previously been shown to yield accurate dynamical results for the H_2+CN reaction. Results presented include integral and differential cross sections, and product vibrational and rotational distributions for ground and vibrational excited HCN. Vector correlations are also discussed. Detailed comparisons with all available experiments are presented, and most of the theoretical results are in excellent agreement with experiment. © *2000 American Institute of Physics.* [S0021-9606(00)00339-1]

I. INTRODUCTION

Although the dynamics of atom+diatom reactions has been extensively studied in the last few years, there have been relatively few attempts to study atom+triatom reactions. One reason for this is the complexity of four atom potential energy surfaces (PES), which are a function of six coordinates. In addition, dynamics methods are more complex for four atom reactions in a variety of ways; for example, the definition of the initial conditions of the triatom often involves a significant calculation in both classical and quantum mechanical studies[1–3] whereas it is relatively easy for diatomics. In this work we present a quasiclassical trajectory (QCT) study of the reaction

$$\mathrm{H+HCN}(\nu_1,\nu_2,\nu_3,j)\rightarrow \mathrm{H_2}(v'_{\mathrm{H_2}},j'_{\mathrm{H_2}})+\mathrm{CN}(v'_{\mathrm{CN}},j'_{\mathrm{CN}}),$$

$$\Delta H^0_{298\,\mathrm{K}}=22.4\pm 0.4\ \ \mathrm{kcal\,mol^{-1}}.^4$$

This represents a continuation of previous studies of the reverse reaction,[5,6] H_2+CN→H+HCN.

The H+HCN reaction has been the subject of significant experimental study in recent years. The work of Carrington and Filseth[7,8] reported experimental data for the reaction of ground state HCN(000) with hot hydrogen atoms at two different translational energies. They photodissociated H_2S and HBr at 193 nm to produce hot H atoms with average translational energies of 53 and 58 kcal $\mathrm{mol^{-1}}$, respectively, relative to the center of mass of the H+HCN system. The resulting cross sections for forming H_2+CN products at these collision energies were 0.007 and 0.009 $\mathrm{Å^2}$, respectively. They also measured the vibrational states of the CN product, and the rotational distributions for the most populated vibrational levels of CN. Johnston and Bersohn[9] obtained hot H atoms from HI photodissociation at 248 nm. A translational energy of 43 kcal $\mathrm{mol^{-1}}$ relative to the H+HCN center of mass is obtained when the H atom corresponds to the ground spin-orbit state of the iodine atom ($\mathrm{I}(^2P_{3/2})$). The excited spin-orbit state is not significant in these studies as the collision energy is lower than the *ab initio* H+HCN reaction barrier (30.5 kcal $\mathrm{mol^{-1}}$ including the zero point energy,[10]). They reported a rotational distribution for CN($v'=0$) which is characterized by an average rotational energy of 1.5 kcal $\mathrm{mol^{-1}}$.

There have also been several experimental studies of the title reaction where the HCN is excited to a specified vibrational state initially. The reaction with four quanta of vibrational excitation in the HCN C–H stretch mode (HCN(004)) was studied by Pfeiffer *et al.* with thermal H atoms.[11] Vibrational populations of the CN product were determined, together with the average CN rotational energy. Kreher *et al.*[12] also measured the rovibrational distributions of the CN generated in the HCN(004) reaction with thermal H atoms, along with hot H atoms with a translational energy of 19 kcal $\mathrm{mol^{-1}}$. Although they could measure the CN internal state distributions arising from the reaction with chlorine atoms when exciting both the CH and CN stretch modes of the HCN ((302) state), no quantitative data are available for the same initial state of HCN with H atoms. Nevertheless, they estimated a ratio between the rate constants for H+HCN(004) and H+HCN(302) of $k(\mathrm{HCN}(004))/k(\mathrm{HCN}(302))>4$. Very recent studies from this group[13] have reported the rovibrational populations of the CN generated in the H+HCN(002) reaction with $E_T=19$ kcal $\mathrm{mol^{-1}}$. The influence of rotational excitation of the parent HCN(004) molecule on the CN rotational populations was also considered. There are also available studies of the stereodynamics of the H+HCN reaction including vibrational and rotational excitation of HCN.[13,14]

There have been very few theoretical attempts to characterize the dynamics of this reaction. Clary[15] obtained in an approximate quantum mechanical (QM) study, the rotational

distributions of the CN product with HCN in the (000), (010), (020), (002) and (004) states. The study was restricted to a total angular momentum equal to zero. The potential energy surface used there was a simple LEPS expression which does not describe geometries other than the collinear (HHCN) one. Kreher *et al.*[13] performed collinear QCT calculations with the LEPS PES derived in Ref. 16. The excitation functions for the H+HCN reaction with different levels of stretching excitation in the reagent HCN were calculated. They also reported CN vibrational populations at collisional energies and initial HCN states where experimental vibrational populations were available.

In this paper we present the results of extensive QCT calculations for the title reaction. This study is based on surface 3 of ter Horst *et al.* (TSH3),[5] which was derived from high quality *ab initio* calculations (multireference configuration interaction methods using correlation consistent basis sets ranging from polarized double zeta to polarized quadruple zeta quality). This surface has already been used in extensive QCT studies of the $H_2+CN \rightarrow H+HCN$ reaction, where good agreement with experiment was generally noted.[5,6,17] These experimental comparisons include thermal rate coefficients (generally in agreement within a factor of 2), product translational energy partitioning data (where both theory and experiment predict that 40% of the available energy ends up as product translational energy) and product angular distributions (backward peaked, with theory being somewhat broader than experiment). Although the experiments of interest for H+HCN are not trivially related by microscopic reversibility to those for H_2+CN, this past work gives us confidence that the present studies should yield accurate results. Only the H_2+CN product of the H+HCN reaction will be considered here, but, of course, other products are possible, and will be discussed elsewhere.

The work is organized as follows: Sec. II deals with the potential energy surface and computational details. Section III considers the HCN ground state reaction. Section IV reports results for reaction involving excited vibrational states of HCN, especially the states (002), (302) and (004). Finally, Sec. V will present some conclusions of this work. Comparison with experimental results is considered where available.

II. POTENTIAL ENERGY SURFACE AND COMPUTATIONAL DETAILS

In this work the more complete PES expression of Ref. 5 (version 3 of that paper, which we denote TSH3) has been used to carry out dynamics calculations with the QCT method. This PES is based on high quality *ab initio* results, and it describes all the important reaction paths available to H+HCN at energies up to about 2 eV. These include the abstraction reaction path to form H_2+CN, which takes place over the collinear HHCN saddle point, and pathways for formation of H_2CN and cis/trans HCNH minima. The PES also describes the reaction channels leading to H+HNC, but study of this product will not be discussed here. The TSH3 PES presents a $H+HCN \rightarrow H_2+CN$ reaction barrier of $24.5\,\mathrm{kcal\,mol^{-1}}$, and a reaction endoergicity of $21.3\,\mathrm{kcal\,mol^{-1}}$. These are to be compared with an experimental endoergicity of 23.2 kcal/mol[5] and a difference between the barrier height and endoergicity which matches experiment to within 0.5 kcal/mol. The H_2CN minimum is $30.8\,\mathrm{kcal\,mol^{-1}}$ below the reactants and there is a barrier of $3.7\,\mathrm{kcal\,mol^{-1}}$ for forming it from H+HCN. The path for forming H_2CN is not connected to that for forming H_2+CN, but H_2CN can still serve as a reaction intermediate by surmounting ridges on the surface. The importance of this process will be assessed in this study.

All the trajectories were started at an initial distance of 10 bohrs between the attacking H atom and the HCN center of mass. The maximum sampling impact parameters were at least 0.5 bohr larger than the maximum impact parameter leading to reaction in each single calculation. The integration step, five time atomic units, was small enough to ensure conservation of both total energy and total angular momentum in the integration to four or more significant figures. A typical reactive trajectory at 6 kcal/mol translational energy is 1000 time steps in duration, but a few that form long lived H_2CN complexes last for as many as 100 000 time steps. The low reactivity of the system and the great variety of initial conditions computed to compare with available experimental data made it necessary to integrate over three million trajectories. Two million trajectory calculations were used for the HCN ground state calculations, and for each excited vibrational state, the analysis has been performed at least with 500 reactive trajectories.

The number of trajectories integrated is such that statistical uncertainties (one standard deviation) for the averaged properties are below 10%. Uncertainties become larger for binned properties (e.g., differential cross sections) and for vibrational state specific properties such as the rotational populations for each vibrational level. These uncertainties have been omitted in most figures, but are presented in the tables.

Comparison with experimental data has required a careful definition of the fractions of the available energy which end up in internal energy of each diatomic. This definition is based on the following expression for the diatomic internal energy:

$$E_{vj} = \omega_e(v+\tfrac{1}{2}) - \omega_e x_e(v+\tfrac{1}{2})^2 + b_e(j)(j+1) - c_e[(j)(j+1)]^2 - e_e(v+\tfrac{1}{2})(j)(j+1).$$

We now divide this into vibrational and rotational energies. In order to make contact with the way the experimentalists define energies, we have subtracted out the zero point energy. This means that the average vibrational energy is defined as

$$\langle E_{\mathrm{VIB}} \rangle = \sum_{v=0}^{v_{\max}} P(v)\,[v\ \omega_e - v(v+1)\ \omega_e x_e]$$

and the average rotational energy is

$$\langle E_{\mathrm{ROT}} \rangle = \sum_{j=0}^{j_{\max}} P(j)\,E_{\mathrm{ROT},j},$$

where

$$E_{\mathrm{ROT},j} = b_e(j)(j+1) - c_e[(j)(j+1)]^2 - e_e(v+\tfrac{1}{2})(j)(j+1).$$

TABLE I. Dependence of some scalar properties on collisional energy for the H+HCN(000,$j=12$) →H_2+CN reaction.

E_T/eV (kcal mol^{-1})	1.865 (43)	2.298 (53)	2.515 (58)	3.000 (69)
σ_r /Å^2	0.008±0.001	0.016±0.001	0.021±0.001	0.026±0.001
Reactivity through H_2CN/%	3.4±0.2	7.0±0.4	8.2±0.4	14.1±0.6
f'_T[a]	0.582±0.028	0.566±0.021	0.584±0.020	0.569±0.019
f'_V(HH)[a]	0.103±0.006	0.164±0.008	0.140±0.006	0.178±0.008
f'_R(HH)[a]	0.243±0.011	0.209±0.009	0.217±0.008	0.203±0.008
f'_V(CN)[a]	0.017±0.001	0.019±0.001	0.020±0.001	0.016±0.001
f'_R(CN)[a]	0.055±0.002	0.044±0.002	0.039±0.001	0.034±0.001
$\langle v'(\mathrm{HH})\rangle$	0.18±0.01	0.42±0.02	0.41±0.02	0.69±0.03
$\langle j'(\mathrm{HH})\rangle$	5.12±0.23	5.93±0.28	6.55±0.28	7.38±0.30
$\langle v'(\mathrm{CN})\rangle$	0.07±0.01	0.10±0.01	0.13±0.01	0.14±0.01
$\langle j'(\mathrm{CN})\rangle$	13.16±0.53	14.24±0.62	14.50±0.59	15.24±0.66
$\langle E_{\mathrm{INT}}(\mathrm{HH})\rangle$/kcal mol^{-1}	7.71±0.39	12.03±0.53	13.31±0.57	18.50±0.77
$\langle E_{\mathrm{VIB}}(\mathrm{HH})\rangle$/kcal mol^{-1}	2.29±0.11	5.29±0.25	5.21±0.22	8.65±0.36
$\langle E_{\mathrm{ROT}}(\mathrm{HH})\rangle$/kcal mol^{-1}	5.42±0.25	6.74±0.30	8.10±0.34	9.85±0.41
$\langle E_{\mathrm{INT}}(\mathrm{CN})\rangle$/kcal mol^{-1}	1.60±0.08	2.03±0.10	2.21±0.10	2.43±0.10
$\langle E_{\mathrm{VIB}}(\mathrm{CN})\rangle$/kcal mol^{-1}	0.37±0.02	0.60±0.03	0.74±0.03	0.79±0.04
$\langle E_{\mathrm{ROT}}(\mathrm{CN})\rangle$/kcal mol^{-1}	1.23±0.06	1.43±0.06	1.47±0.07	1.64±0.07
E_{avail}[a]/kcal mol^{-1}	22.30	32.30	37.30	48.48

[a]$E_{\mathrm{avail}}=E_T+E_{\mathrm{INT}}-\Delta H^0_{0\ \mathrm{K}}$, with $E_{\mathrm{INT}}=E_{\mathrm{VIB}}+E_{\mathrm{ROT}}$, and $E_{\mathrm{ROT}}=B_e(j)(j+1), j=12$.

The average fractions of energy ending up as vibration and rotation are the ratios of the average vibrational and rotational energy to the (zero point energy subtracted) total energy, respectively.

The choice of initial rotational states in the reagent HCN molecule has also been considered. At 300 K the most probable rotational level of HCN is 8, and the average rotational level is 12. We have used the average rotational level $j(\mathrm{HCN})=12$ to simulate a room temperature distribution of rotational levels. In the HCN vibrationally excited states study, j(HCN) has been fixed equal to 9 to be consistent with the experiments of Gericke *et al.*[12–14] where HCN was mainly prepared in this state.

It's also important to define the scattering angle in this work. For a three atom system, the scattering angle is defined as the angle between the initial relative velocity vector **k** and the final relative velocity vector **k′**. The latter vector is defined to point toward the direction of the newly formed diatom which includes the attacking atom. For an atom+triatom→diatom+diatom system, the consistent way to define the sense of **k′** would be toward the newly formed diatom which contains the attacking atom. But this newly formed diatom (H_2) is experimentally difficult to measure for H+HCN; instead it is the diatom whose bond was already present in the reagent HCN (CN) that has been studied. Thus we take the scattering angle such that **k′** points to the

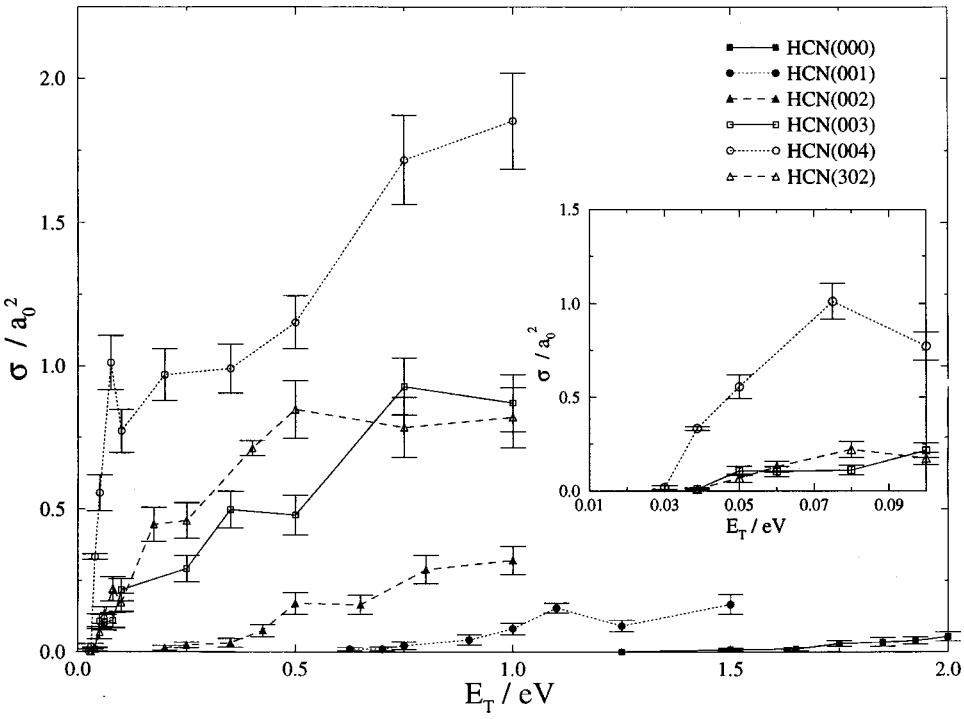

FIG. 1. Excitation function (integral cross section vs translational energy) for the H+HCN(ν_1,0,ν_3,j)→H_2 +CN reaction. $j(\mathrm{HCN})=12$ for HCN(000) and $j(\mathrm{HCN})=9$ for the other states.

CN product. This definition has been previously used for $H+H_2O$.[18]

All the QCT results have been computed by omitting reactive trajectories for which the H_2 vibrational energy is below the zero point energy. The CN product vibrational energy is not constrained. This procedure (i.e., constraining only the newly formed bond) was successfully considered for the $H+H_2O$ system in a previous work,[18] and an analogous procedure was found to work well in the H_2+CN reaction.[6]

III. H+HCN(000)→H_2+CN

A. Cross sections

We begin by considering the reaction of translationally hot hydrogen atoms with ground state HCN. Table I presents cross sections and product energy partitioning information for the ground state reaction at four translational energies, three of them (43, 53 and 58 kcal mol^{-1}) matching the values that have been considered in experiment. The cross sections for H+HCN(000), as well as for several other states of HCN, are plotted in Fig. 1. This shows, as expected,[19] that the threshold energy for the ground state reaction is very high (>1.25 eV), and the cross section is very low even at energies well above threshold. This threshold drops considerably and the cross section increases for vibrationally excited HCN, but we will defer a discussion of this until later.

The ground state cross sections in Table I and Fig. 1 are similar in magnitude and energy dependence to what one finds for other direct endoergic abstraction reaction like $H+H_2O$.[18] This is, of course, expected,[19] given that the barrier is located in the product region of the potential surface. However, some of the reaction probability comes from the insertion elimination mechanism. This can be seen in the entry ''Reactivity through H_2CN'' of Table I, which accounts for about 15% of the cross sections at high energy.

To further study the results in Table I and Fig. 1, we consider comparisons with experiment. The cross sections for $E_T=53$ and 58 kcal mol^{-1} were experimentally determined in Ref. 8. The experimental values obtained there were 0.007 ± 0.002 and 0.009 ± 0.002 Å^2, for 53 and 58 kcal mol^{-1}, respectively. These values are about half of the trajectory values, 0.016 ± 0.001 and 0.021 ± 0.001 Å^2, respectively. This level of agreement (i.e., factor of 2) is similar to what has been obtained in past comparisons between theory and experiment for $H+H_2O$ (Ref. 18) for cross sections that are of the same order of magnitude, and it is probably as good as can be expected given the strong sensitivity of the results to the zero point constraint for this property (which we infer based on detailed results for $H+H_2O$,[18] and on the work of Bethardy and co-workers[6] for the reverse reaction), and to the quality of the potential surface (as analyzed by ter Horst *et al.*[5] who considered several possible surfaces for the reverse reaction).

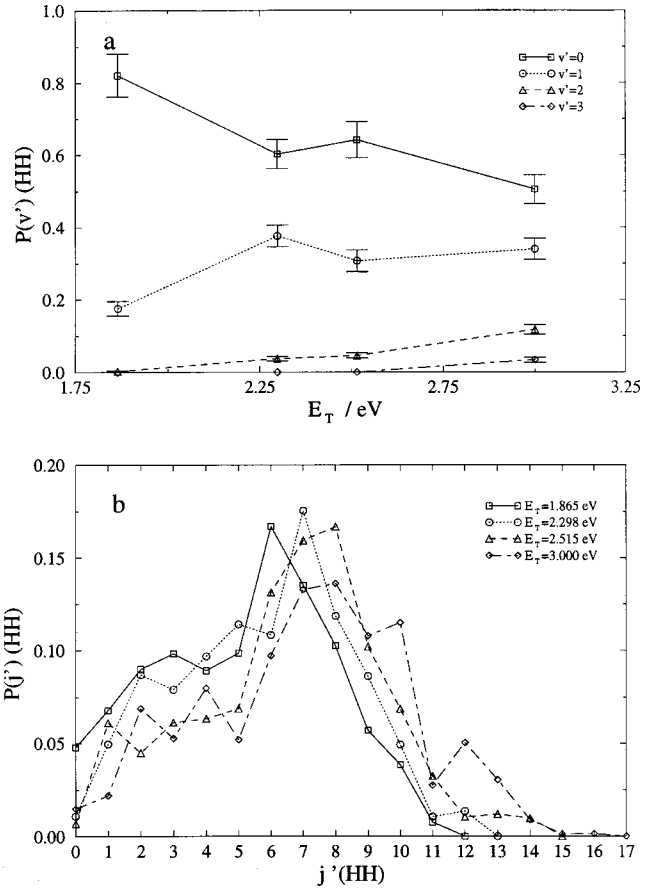

FIG. 2. H+HCN(000,$j=12$)→$H_2(v',j')$+CN reaction: (a) H_2 vibrational populations; (b) $H_2(v'=0)$ rotational populations. All the populations are normalized to unity.

B. Vibrational and rotational distributions

Results for the ground state reaction concerning the H_2 vibrational and rotational distributions are presented in Table I and Fig. 2. The CN internal distributions are also shown in

TABLE II. Experimental and QCT CN vibrational populations and average fractions of vibrational energy for the H+HCN(000,$j=12$)→H_2+CN(v') reaction, with $E_T=43$, 53 and 58 kcal mol^{-1}.

	E_T/eV (kcal mol^{-1})	$P(v'=0)$	$P(v'=1)$	$P(v'=2)$	f'_V(CN)[a]
Exp. (Ref. 9)	1.865 (43)	1	0		
QCT	1.865 (43)	0.936 ± 0.061	0.064 ± 0.010		0.028 ± 0.001
Exp. (Ref. 8)	2.298 (53)	0.866 ± 0.005	0.134 ± 0.005		0.032 ± 0.001
QCT	2.298 (53)	0.898 ± 0.058	0.102 ± 0.014		0.026 ± 0.002
Exp. (Ref. 8)	2.515 (58)	0.81 ± 0.03	0.14 ± 0.01	0.05 ± 0.03	0.047 ± 0.008
QCT	2.515 (58)	0.880 ± 0.046	0.113 ± 0.013	0.007 ± 0.002	0.026 ± 0.002

[a]Here, the calculations of the QCT average fractions of energy have considered the same nonstandard available energy as the one considered in the experiments, $E_{avail}=E_T-30$ (kcal mol^{-1}).

TABLE III. Experimental and QCT CN rotational data for the H+HCN(000,$j=12$)→H_2+CN reaction.

	E_T/eV (kcal mol^{-1})	T_{ROT}/K	$\langle E_{ROT}\rangle$/kcal mol^{-1}	j'_{mp}
Exp. (Ref. 9), $v'=0$	1.865 (43)	760±35	1.51±0.07	12
QCT, $v'=0$	1.865 (43)		1.24±0.06	12
Exp. (Ref. 8), $v'=0$	2.298 (53)	1404±95	2.78±0.19	16
QCT, $v'=0$	2.298 (53)		1.48±0.10	15
Exp. (Ref. 8), $v'=0$	2.515 (58)	1626±40	3.22±0.08	17
QCT, $v'=0$	2.515 (58)		1.47±0.09	14
Exp. (Ref. 8), $v'=1$	2.298 (53)	1430±391	2.83±0.78	16
QCT, $v'=1$	2.298 (53)		1.35±0.20	12
Exp. (Ref. 8), $v'=1$	2.515 (58)	1645±137	3.26±0.27	17
QCT, $v'=1$	2.515 (58)		1.57±0.18	12

Table I. Comparison with experiment is available in Table II (CN vibration), and in Table III and Fig. 3 (CN rotation). These data show that the average energy in H_2 vibration increases with E_T such that the corresponding average fraction of energy is moderate (10%) at 43 kcal mol^{-1} while that at 69.2 kcal mol^{-1} is among the largest of the average fractions of internal energy (18%). By contrast, the average CN vibrational energy is small and essentially independent of translational energy, such that the average fraction of CN vibrational energy is nearly constant at about 1.8% of the available energy (Table I). The energy in H_2 and CN rotation increases slowly with translational energy, with the average fraction of rotational energy being roughly constant at 22% for H_2 and 4% for CN.

Comparison between theory and experiment[8,9] is possible for the CN vibrational populations at $E_T=43$, 53 and 58 kcal mol^{-1}. These results (Table II) show good agreement between theory and experiment, with the CN molecule having little excitation. This excitation increases slowly with energy, but if we examine Table I, we see that this increase is slower than the increase in available energy so that the fraction of energy in CN vibration decreases with energy.

Comparisons with experiment may also be made for the CN rotational distributions. These are shown in Table III, and in Fig. 3. The CN rotational distributions in the CN($v'=0$) state were measured for 43[9], 53 and 58[8] kcal mol^{-1}, while the rotational distributions of CN($v'=1$) were measured at 53 and 58[8] kcal mol^{-1}. These rotational distributions were well fitted to Maxwell-Boltzmann distributions, thus giving the CN rotational temperatures, the CN average rotational energies, and the average fractions of the available energy going into CN rotation. Table III shows the QCT and experimental data available for CN rotation arising from reaction with HCN in the ground state, including the most probable CN rotational level (j'_{mp}).

The measured average fractions of CN rotational energy, considering a nonstandard available energy defined as E_T-30 kcal mol^{-1}, are 0.11±0.01,[9] 0.12±0.01 and 0.12±0.01[8] for $E_T=43$, 53 and 58 kcal mol^{-1}, respectively. The QCT results for the lowest translational energy considered are in very good agreement with the experiment (0.09±0.01), while the QCT results for 53 and 58 kcal mol^{-1} (0.06±0.01 and 0.05±0.01, respectively) are somewhat colder than the experimental data. Figure 3 plots the experimental and QCT CN($v'=0$) rotational distributions. The experimental distributions, that correspond to Maxwell–Boltzmann fits, are characterized by the rotational temperatures of Table III.

As can be seen in Table III and Fig. 3, despite the rather good agreement of the experimental and QCT CN($v'=0$) rotational distributions for $E_T=43$ kcal mol^{-1}, the QCT ones for the larger collisional energies are not in good agreement with experiment. Although the peaks of the QCT and experimental rotational distributions are close for 53 and 58 kcal mol^{-1}, the experimental distributions are hotter than

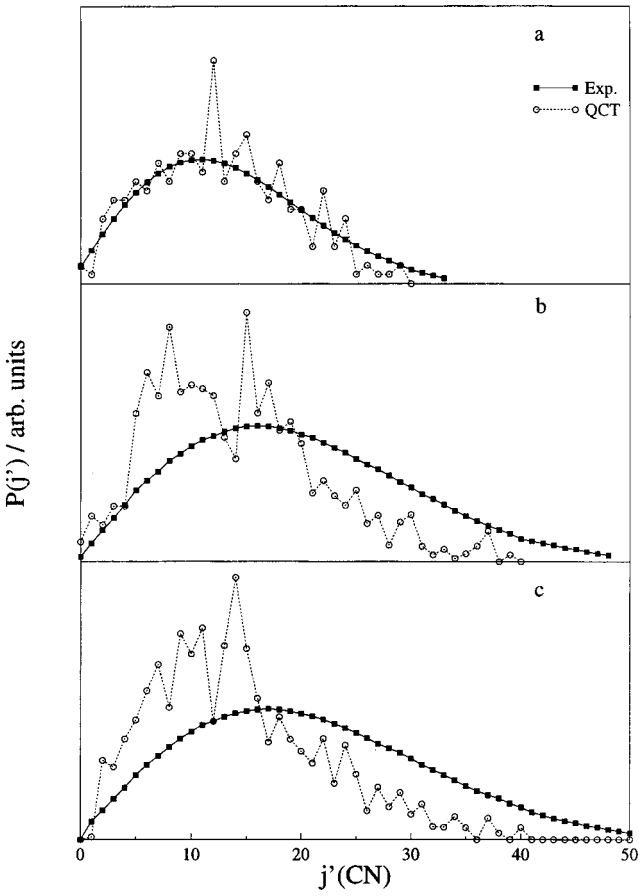

FIG. 3. Experimental and QCT CN($v'=0$) rotational populations for the H+HCN(000,$j=12$)→H_2+CN reaction with $E_T=43$ (a), 53 (b) and 58 (c) kcal mol^{-1}. All the distributions have been normalized to unity for the common j'(CN) values.

TABLE IV. Average two-vector properties for the H+HCN(000,$j=12$)→H_2+CN reaction.

E_T/eV (kcal mol^{-1})	1.865 (43)	2.298 (53)	2.515 (58)	3.000 (69)
$\langle \mathbf{kk}'\rangle$[a] / deg.	76.5±3.5	86.7±3.8	89.3±3.8	96.2±4.0
f/b ratio	2.01±0.10	1.28±0.06	0.98±0.05	0.61±0.03
$\mathbf{kk}'$ $A_0^{(1)}$	0.21±0.01	0.05±0.01	0.01±0.01	−0.10±0.01
$\mathbf{kk}'$ $A_0^{(2)}$	−0.07±0.01	−0.27±0.02	−0.25±0.02	−0.35±0.02
$\langle \mathbf{j}'\mathbf{j}'\rangle$ / deg.	86.2±3.9	86.1±3.8	80.9±3.4	81.3±3.6
p/ap ratio	1.23±0.06	1.16±0.06	1.50±0.07	1.42±0.07
$\mathbf{j}'\mathbf{j}'$ $A_0^{(1)}$	0.07±0.01	0.07±0.01	0.13±0.01	0.13±0.01
$\mathbf{j}'\mathbf{j}'$ $A_0^{(2)}$	0.20±0.01	0.13±0.01	0.21±0.01	0.00±0.01

[a]Here $\mathbf{k}'$ has been defined to point toward the CN product (see text).

the QCT distributions. The experimental average rotational energies are about two times larger than the QCT ones, and the increase in CN rotational excitation with increasing collisional energy is more gradual in the QCT calculations than in the experiments.[8,9] Moreover, the CN rotational excitation does not appear to decrease with increasing vibrational excitation (Table III), as is generally observed in triatomic reactions. A strong, positive correlation between rotation and vibration is not observed either; instead the amount of rotational excitation in the experimental and QCT CN vibrational levels studied for 53 and 58 kcal mol^{-1} is approximately constant. A positive vibration-rotation correlation has never been observed in the atom+diatom systems, and it is thought that its appearance in atom+triatom(polyatom) reactions[20] reflects their greater complexity. The high rotational excitation of CN together with the moderate energy disposal in CN vibration, are therefore indications of the nonspectator behavior of the CN product.

C. Vector correlations

To provide deeper insight into the reaction dynamics, we have studied the two-vector properties associated with the $\mathbf{kk}'$, $\mathbf{kj}'_{HH}$, $\mathbf{kj}'_{CN}$, $\mathbf{k}'\mathbf{j}'_{HH}$, $\mathbf{k}'\mathbf{j}'_{CN}$ and $\mathbf{j}'_{HH}\mathbf{j}'_{CN}$ angles. Here $\mathbf{k}$ is the initial relative velocity vector, $\mathbf{k}'$ the products relative velocity vector already defined to point toward the CN product, $\mathbf{j}'_{HH}$ the rotational angular momentum vector associated with the H_2 product and $\mathbf{j}'_{CN}$ the CN rotational angular momentum vector.

A brief analysis of the two-vector average properties (Table IV) and angular distributions in terms of differential cross sections (DCS) is presented in Fig. 4. Since the scat-

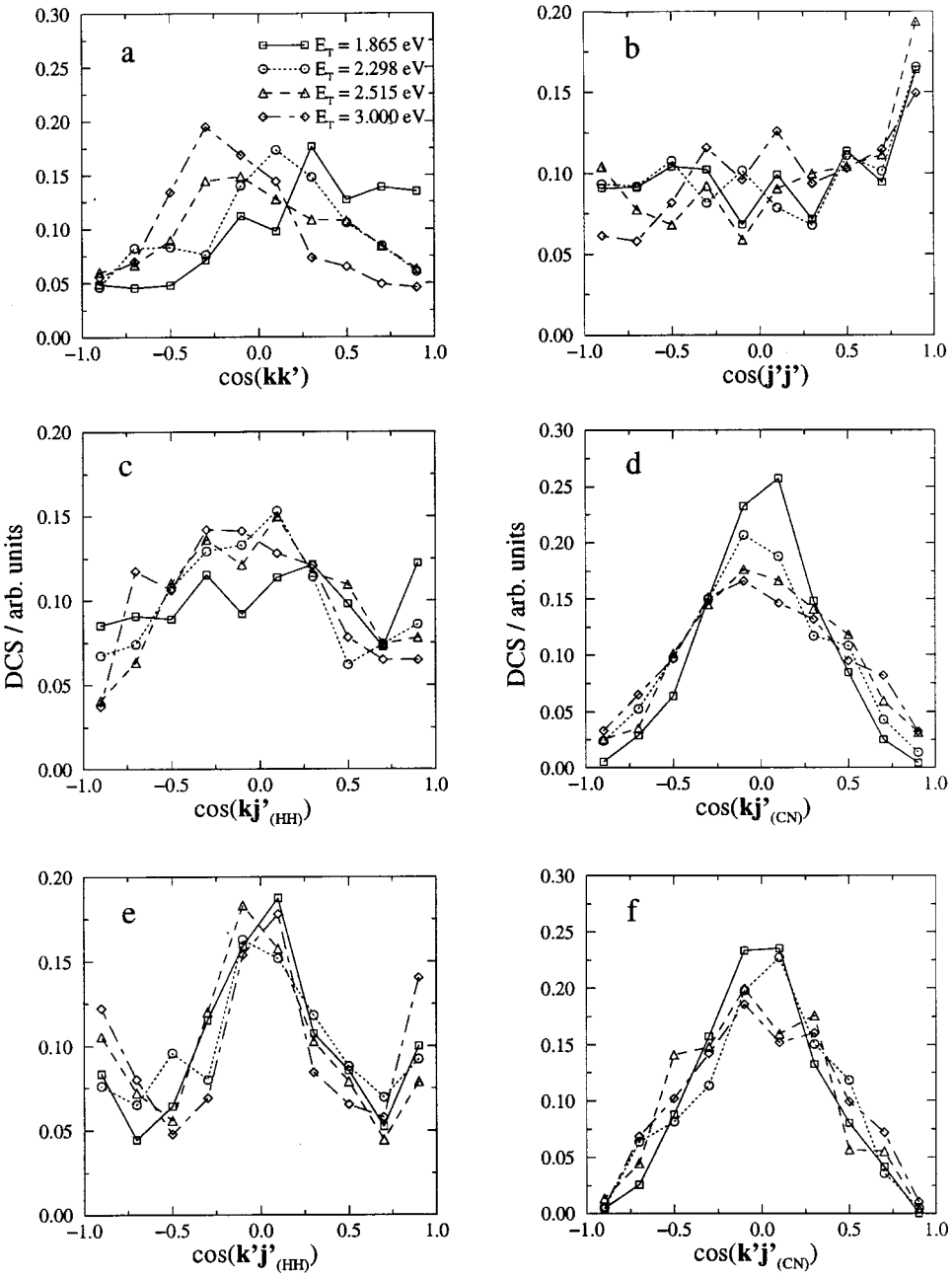

FIG. 4. Differential cross sections (DCS) for the H+HCN(000,j=12) $\rightarrow$H$_2$+CN reaction. All the DCS have been normalized to unity.

TABLE V. Scalar properties for the H+HCN(ν_1,0,ν_3,$j=9$)→H_2+CN reaction, $E_T=0.83$ eV.

HCN state	002	302	004
σ_r /Å^2	0.082±0.003	0.241±0.010	0.413±0.017
Reactivity through H_2CN/%	0.7±0.4	1.5±0.1	1.2±0.1
$f_T'^{a}$	0.571±0.021	0.394±0.015	0.422±0.017
f_V'(HH)[a]	0.133±0.006	0.209±0.010	0.234±0.011
f_R'(HH)[a]	0.201±0.009	0.190±0.009	0.231±0.011
f_V'(CN)[a]	0.047±0.002	0.186±0.008	0.091±0.006
f_R'(CN)[a]	0.048±0.002	0.021±0.001	0.022±0.001
$\langle v'(\mathrm{HH})\rangle$	0.17±0.01	0.56±0.02	0.63±0.03
$\langle j'(\mathrm{HH})\rangle$	4.04±0.17	5.70±0.24	6.40±0.31
$\langle v'(\mathrm{CN})\rangle$	0.13±0.01	1.08±0.05	0.53±0.02
$\langle j'(\mathrm{CN})\rangle$	9.83±0.42	9.35±0.41	9.57±0.39
$\langle E_{\mathrm{INT}}(\mathrm{HH})\rangle$/kcal mol^{-1}	5.52±0.29	13.54±0.55	15.79±0.64
$\langle E_{\mathrm{VIB}}(\mathrm{HH})\rangle$/kcal mol^{-1}	2.20±0.13	7.09±0.29	7.96±0.32
$\langle E_{\mathrm{ROT}}(\mathrm{HH})\rangle$/kcal mol^{-1}	3.32±0.18	6.45±0.26	7.83±0.31
E_{avail}[a]/kcal mol^{-1}	16.5	33.96	33.96

[a]$E_{\mathrm{avail}}=E_T+E_{\mathrm{INT}}-\Delta H^0_{0\,\mathrm{K}}$, with $E_{\mathrm{INT}}=E_{\mathrm{VIB}}+E_{\mathrm{ROT}}$, and $E_{\mathrm{ROT}}=B_e(j)(j+1), j=9$.

tering angle is referred to the CN product ($\mathbf{kk}'$), a rebound mechanism would be expected to give predominantly forward scattering, and this is what we see in Fig. 4(a) at low energies. In addition, we see that the average angle, forward/backward scattering ratio (cross section of the trajectories scattered into the forward hemisphere over the cross section for scattering into the backward one) and orientation parameter ($A_0^{(1)}=\langle\cos(\mathbf{kk}')\rangle$) show that the $\mathbf{kk}'$ angular distribution tends to be less forward with increasing E_T [Table IV and Fig. 4(a)]. The coefficients $A_0^{(1)}$ and $A_0^{(2)}$ [alignment parameter $A_0^{(2)}=\langle 3\cos^2(\mathbf{kk}')-1\rangle$], have the usual definitions.[21,22] $A_0^{(1)}$ can range from $+1$ for parallel distributions, to -1 for antiparallel distributions, having the value of 0 for perpendicular distributions. $A_0^{(2)}$ ranges from $+2$ for parallel and antiparallel distributions to -1 for perpendicular distributions.

The $\mathbf{j}'\mathbf{j}'$ angular distributions [Table IV and Fig. 4(b)] show a preference for more parallel distributions with increasing E_T. This suggests that the collision process has some tendency toward planarity. Planar configurations correspond to the minimum energy path in the TSH3 PES, as well as to the H_2CN minimum (which contributes to the dynamics at high energy). All the $\mathbf{kj}'$ and $\mathbf{k}'\mathbf{j}'$ distributions peak at 90 degrees and are symmetric about 90 degrees. There is not a clear tendency to broaden or narrow with E_T in the case of the $\mathbf{kj}'_{\mathrm{HH}}$ and $\mathbf{k}'\mathbf{j}'_{\mathrm{HH}}$ angular distributions [Figs. 4(c) and 4(e), respectively]. However, there is some broadening with increasing E_T in the case of the $\mathbf{kj}'_{\mathrm{CN}}$ and $\mathbf{k}'\mathbf{j}'_{\mathrm{CN}}$ angular distributions [Figs. 4(d) and 4(f), respectively].

Based on the results described above we find that the strongest variation with E_T occurs for the $\mathbf{kk}'$ angular distribution.

IV. H+HCN(ν_1,0,ν_3)→H_2+CN

This section deals with the effect of the vibrational excitation on the cross sections, and on the properties of the H_2 and CN products. Three states of HCN that have been the subject of several recent experimental studies will be emphasized here: (002), (302) and (004). The latter two states have nearly the same energy, so a comparison of results for these indicates the importance of mode specificity in the reaction dynamics. By contrast, comparisons between (002) and (302) show the effect of CN stretch mode excitation, while (002) and (004) show the effect of CH stretch mode excitation.

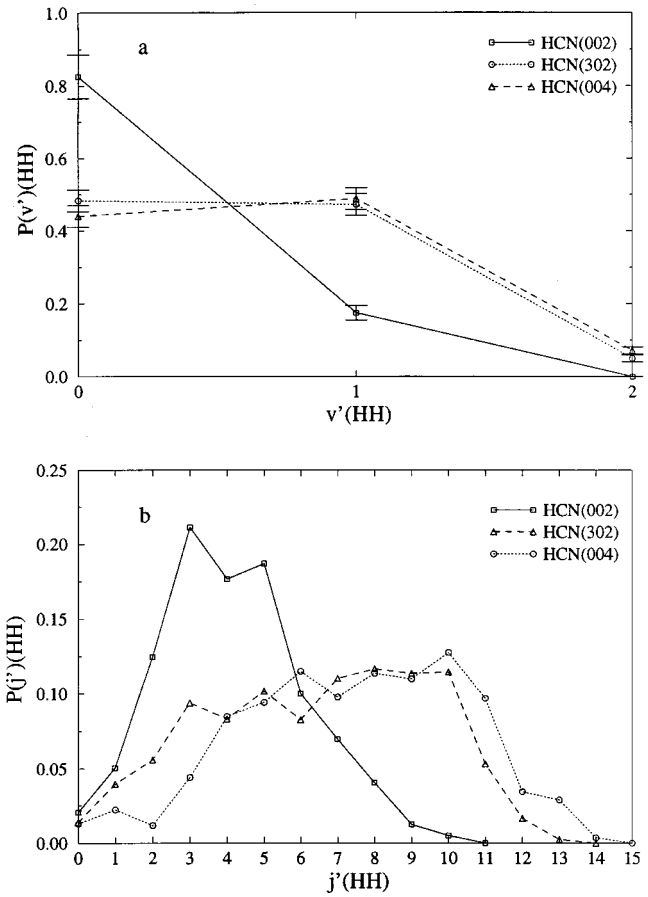

FIG. 5. H+HCN(ν_1,0,ν_3,$j=9$)→H_2(v',j')+CN reaction: (a) H_2 vibrational populations; (b) H_2($v'=0$) rotational populations. All the populations are normalized to unity. $E_T=0.83$ eV.

A. Excitation functions and product energy distributions

The excitation functions associated with several states of HCN are plotted in Fig. 1. This shows that excitation of the CH stretch mode of HCN leads to substantial reduction in reactive threshold energies compared to the ground state, along with much larger cross sections. Figure 1 therefore shows that vibrational excitation is much more efficient than translational energy for increasing reactivity. This is what is to be expected for a system with a late barrier.[19] The threshold energy reduction is especially large for the progression of states (000), (001), (002) and (003), dropping from >1.25 eV to 0.04 eV. (302) has about the same threshold energy as (003), and the (004) threshold is 0.03 eV. This threshold energy behavior is similar to what several of us found in recent studies of H+H_2O (Ref. 23) [considering the states (000), (001), (002), (003) and (004)] except that the threshold energy for (003) and (004) is zero for the best

TABLE VI. Scalar properties for the H+HCN(ν_1,0,ν_3,$j=9$)→H_2+CN reaction, $E_T=0.4$ eV.

HCN state	002	302	004
σ_r /Å^2	0.023±0.001	0.199±0.007	0.328±0.011
Reactivity through H_2CN/%	0	0.1±0.1	1.0±0.1
f'_T[a]	0.739±0.026	0.327±0.013	0.286±0.011
f'_V(HH)[a]	0.052±0.002	0.300±0.012	0.368±0.014
f'_R(HH)[a]	0.151±0.005	0.157±0.006	0.208±0.009
f'_V(CN)[a]	0.005±0.001	0.190±0.007	0.113±0.005
f'_R(CN)[a]	0.053±0.002	0.026±0.001	0.025±0.001
$\langle v'(\mathrm{HH})\rangle$	0.03±0.01	0.55±0.02	0.68±0.02
$\langle j'(\mathrm{HH})\rangle$	2.05±0.09	4.10±0.14	4.90±0.17
$\langle v'(\mathrm{CN})\rangle$	0.01±0.01	0.75±0.03	0.45±0.02
$\langle j'(\mathrm{CN})\rangle$	6.87±0.28	8.66±0.29	8.41±0.28
E_{avail}[a]/kcal mol^{-1}	6.59	23.10	23.10

[a]$E_{\mathrm{avail}}=E_T+E_{\mathrm{INT}}-\Delta H^0_{0\,\mathrm{K}}$, with $E_{\mathrm{INT}}=E_{\mathrm{VIB}}+E_{\mathrm{ROT}}$, and $E_{\mathrm{ROT}}=B_e(j)(j+1), j=9$.

potential surfaces rather than being the small values found here (<0.04 eV). The H+H_2O study demonstrated substantial sensitivity of this threshold energy to the shape of the potential surface for geometries where the excited O–H bond in H_2O is near its outer turning point. Since the potential surface used for the present studies was not optimized for large C–H stretch displacements, it is possible that the surface is not accurate when dealing with the threshold energy for this type of displacement, and that the cross section should have a zero energy threshold rather than the values below 0.04 eV.

To get a more complete description of the effect of the HCN vibrational excitation, Table V gives some scalar properties for H+HCN in the states (002), (302) and (004) for a translational energy of 0.83 eV (the average energy studied in experiments when CH_3SH is photolyzed at 266 nm) and an initial rotational level of HCN equal to 9. This table shows that the cross section for the HCN(004) state is the largest one, being almost two times the HCN(302) result, in spite of the fact that the total energy for these two states is the same. This suggests that the C–H mode is more efficiently coupled with the reaction coordinate than the C–N mode. Note also that the HCN(002) state cross section is three times smaller than the one for HCN(302). This difference might be due to the larger total energy of HCN(302) relative to HCN(002) (around two times larger), and this result also indicates that although the C–N stretching mode is not as strongly coupled to the reaction coordinate as C–H, it is not completely uncoupled either.

TABLE VII. Scalar properties for the H+HCN(ν_1,0,ν_3,$j=9$)→H_2+CN, $E_T=1.865$ eV, reaction.

HCN state	002	302	004
σ_r /Å^2	0.170±0.007	0.229±0.010	0.399±0.018
Reactivity through H_2CN/%	2.4±0.1	3.0±0.2	2.4±0.1
f'_T[a]	0.512±0.022	0.400±0.018	0.455±0.020
f'_V(HH)[a]	0.195±0.007	0.181±0.008	0.211±0.009
f'_R(HH)[a]	0.209±0.007	0.223±0.009	0.251±0.010
f'_V(CN)[a]	0.055±0.002	0.177±0.007	0.065±0.002
f'_R(CN)[a]	0.029±0.001	0.019±0.002	0.018±0.001
$\langle v'(\mathrm{HH})\rangle$	0.62±0.03	0.82±0.04	0.95±0.05
$\langle j'(\mathrm{HH})\rangle$	6.69±0.27	8.53±0.34	9.09±0.38
$\langle v'(\mathrm{CN})\rangle$	0.38±0.02	1.73±0.08	0.63±0.03
$\langle j'(\mathrm{CN})\rangle$	11.97±0.51	10.89±0.49	10.82±0.52
E_{avail}[a]/kcal mol^{-1}	40.38	56.88	56.88

[a]$E_{\mathrm{avail}}=E_T+E_{\mathrm{INT}}-\Delta H^0_{0\,\mathrm{K}}$, with $E_{\mathrm{INT}}=E_{\mathrm{VIB}}+E_{\mathrm{ROT}}$, and $E_{\mathrm{ROT}}=B_e(j)(j+1), j=9$.

TABLE VIII. Experimental and QCT CN vibrational populations and average fractions of internal energy for the H+HCN(002,$j=9$)→H_2+CN(v',j') reaction with $E_T=0.83$ eV.

	$P(v'=0)$	$P(v'=1)$	f'_V(CN)[a]	f'_R(CN)[a]
Exp. (Ref. 13)	0.95	<0.05	0.02	0.06
QCT	0.868±0.053	0.132±0.016	0.046±0.008	0.048±0.008

[a]$E_{\mathrm{avail}}=16.50$ kcal mol$^{-1}=E_T+E_{\mathrm{INT}}-\Delta H^0_{0\,\mathrm{K}}$, with $E_{\mathrm{INT}}=E_{\mathrm{VIB}}+E_{\mathrm{ROT}}$, and $E_{\mathrm{ROT}}=B_e(j)(j+1), j=9$.

Table V shows that H_2 product vibrational excitation depends on the HCN C–H excitation, with values of the average vibrational energy, the average fraction of H_2 vibrational energy and the average vibrational quantum numbers of HCN(302) that are somewhere between HCN(002) and HCN(004), although closer to HCN(004) as can be seen from the very similar H_2 vibrational distributions of Fig. 5(a). The H_2 rotational excitation behavior for the three states is similar to that for vibration, with average rotational energy and average H_2 rotational quantum numbers increasing in going from HCN(002) to HCN(302) and HCN(004). Here the HCN(302) H_2 rotational distribution is reasonably close to the HCN(004) one, as seen in the $H_2(v'=0)$ rotational distributions in Fig. 5(b). Table V also shows that CN vibrational excitation is small for (002), much larger for (302) and in-between for (004), while the average CN rotational quantum number is close to the initial HCN value of 9 for all three states. The values of the average CN vibrational quantum numbers indicate that there is only a rough correlation between the initial C–N stretch quantum number in HCN and that in the CN product.

To study the variation of the results just discussed with translational energy, in Tables VI and VII we present results analogous to Table V but for energies of 0.4 and 1.865 eV. The former energy is not far from the HCN(002) reactive threshold (about 0.2 eV, see Fig. 1) and is representative of this part of the excitation function. The latter energy corresponds to the energy of hot H atoms generated when HI is photodissociated at 248 nm (and yielding ground state I).

The analysis of the cross sections, energy partitioning in products and internal state distributions of the H_2 and CN products reveals that the tendencies observed for $E_T=0.83$ eV are still present at 0.4 and 1.865 eV, but with the expected changes that arise from the lower and higher value of E_T. In particular, the cross section for HCN (002) is very small compared to the others in Table VI ($E_T=0.4$ eV), while all three cross sections are more comparable in Table VII ($E_T=1.865$ eV). The fraction of reaction that proceeds through the H_2CN minimum rises with increasing translational energy, and at 1.865 eV it accounts for about 3% of

TABLE IX. Experimental and QCT CN vibrational populations and average fractions of internal energy for the H+HCN(004,$j=9$)→H_2+CN(v',j') reaction with $E_T=0.0388$ eV.

	$P(v'=0)$	$P(v'=1)$	$P(v'=2)$	f'_V(CN)[a]	f'_R(CN)[a]
Exp. (Ref. 11)	0.77±0.06	0.17±0.06	0.06±0.06	0.107	0.025
Exp. (Ref. 12)	0.60±0.03	0.28±0.03	0.12±0.03	0.192	0.045
QCT	0.62±0.07	0.33±0.04	0.05±0.02	0.159±0.011	0.019±0.001

[a]$E_{avail}=15.78$ kcal mol$^{-1}=E_T+E_{INT}-\Delta H^0_{0\,K}$, with $E_{INT}=E_{VIB}+E_{ROT}$, and $E_{ROT}=B_e(j)(j+1)$,$j=9$.

the reactive trajectories for all three states. The average quantum numbers associated with the H_2 and CN vibrational and rotational motions increase with increasing translational energy. There is a more significant amount of the available energy going into translation for the (002) state than for the (302) and (004) states. Moreover, for the HCN(002) state with $E_T=0.4$ eV only a very small fraction of the available energy is channeled to product internal energy.

B. Comparison with experimental results

The CN vibrational distributions for H+HCN(002) and H+HCN(004) have been experimentally measured. Both thermal (300 K) H atoms and hot H atoms (0.83 eV) were used to react with HCN(004). In the case of the HCN(002) reactions, the thermal H atoms do not have enough translational energy (0.0388 eV) to generate the H_2+CN products so the only CN vibrational distributions are for 0.83 eV collisional energy. Table VIII presents comparisons between theory and experiment[13] for (002) at 0.83 eV. The experiment shows that the CN vibration is relatively cold, with only 2% of the available energy going into CN vibration. The QCT vibrational distributions for the same initial conditions are also cold (5% of the available energy). A closer comparison between theory and experiment is provided by CN rotation, where $\langle E_{ROT}\rangle=1.08$ kcal mol^{-1} in the experiment and 0.79 kcal mol^{-1} in the QCT results.

QCT results for H+HCN(004) with thermal translational energy are compared with experiment[11,12] in Table IX. This shows good agreement between the QCT and experimental CN vibrational populations, with the QCT data somewhere in between the more vibrationally excited values of Ref. 12 and the colder ones of Ref. 11. Moreover, CN rotation is also well described by the QCT calculations. The QCT average rotational energy ($\langle E_{ROT}\rangle=0.31\pm0.01$ kcal mol^{-1}) shows a quite good agreement with the measurements of Ref. 11 ($\langle E_{ROT}\rangle=0.40$ kcal mol^{-1}) and is colder than the rough estimations of Ref. 12 ($\langle E_{ROT}\rangle=0.72$ kcal mol^{-1}).

Table X presents results for H+HCN(004)→H_2+CN(v',j') at 0.83 eV. This shows quite good agreement between the QCT and experimental[12] vibrational populations. The CN product QCT and experimental average rotational energies are also rather close ($\langle E_{ROT}\rangle=0.75\pm0.03$ and 0.91 kcal mol^{-1}, respectively). Tables IX and X allow us to conclude that the PES used in this work is accurate enough to describe high vibrational excitations in the C–H mode of the reagent HCN.

The HCN(302) vibrational state has also been experimentally studied,[13] although there is no available experimental information on the CN rovibrational distributions. Nevertheless, QCT calculations with $E_T=0.83$ eV have been done in this work, to see how excitation of the C–N mode in the reagent HCN affects the internal states of the CN product. The CN vibrational distributions arising from these calculations $[P(v'=0):P(v'=1):P(v'=2):P(v'=3)=0.24\pm0.02:0.50\pm0.03:0.20\pm0.01:0.06\pm0.01]$ are much more excited than the ones corresponding to HCN(002) (see Table VIII) and are also more excited than the ones calculated for HCN(004) (see Table X). On the other hand, the CN average rotational energy (0.72 ± 0.03 kcal mol^{-1}) is very similar to the results for HCN(002) and HCN(004), suggesting that the CN rotational distributions might not be affected by HCN vibrational excitation. The differences between the CN vibrational distributions from the HCN(002) and HCN(004) reactions with $E_T=0.83$ eV (Tables VIII and X, respectively) might be due to the possible channelling of the higher total energy to the CN vibrational mode in the case of the HCN(004) state with respect to the HCN(002) state, showing that the C–N mode is not uncoupled with the modes leading to reaction.

Kreher *et al.*[13] also considered the effect of the rotational excitation of the parent HCN in the CN product rotational distributions for the (004) vibrational state of HCN. They found the expected positive correlation between the rotational excitation of HCN and the product CN rotation. They quantified the results in terms of rotational temperatures by fitting the measured CN rotational distributions to Maxwell–Boltzmann functions. The low QCT statistics in the high excitation wing of the CN rotational distribution does not allow the correct derivation of the rotational temperature of the complete rotational distributions from a fit to Maxwell–

TABLE X. Experimental and QCT CN vibrational populations and fractions of internal energy for the H+HCN(004,$j=9$)→H_2+CN(v',j') reaction with $E_T=0.83$ eV.

	$P(v'=0)$	$P(v'=1)$	$P(v'=2)$	$P(v'=3)$	f'_V(CN)[a]	f'_R(CN)[a]
Exp. (Ref. 12)	0.53±0.03	0.33±0.03	0.14±0.03		0.10	0.03
QCT	0.62±0.04	0.25±0.02	0.11±0.02	0.02±0.01	0.091±0.004	0.022±0.001

[a]$E_{avail}=33.96$ kcal mol$^{-1}=E_T+E_{INT}-\Delta H^0_{298\,K}$, with $E_{INT}=E_{VIB}+E_{ROT}$, $E_{ROT}=B_e(j)(j+1)$,$j=9$.

TABLE XI. Experimental and QCT rotational data for the $H+HCN(004,j)\rightarrow H_2+CN(v'=0,j')$ reaction, $j=2$, 9, 16. $E_T=0.83$ eV.

	j(HCN)	T_{ROT}/K	$\langle E_{ROT}\rangle$	j'_{mp}
Exp. (Ref. 13)	2	490±34	0.98±0.07	9±1
QCT	2		0.53±0.03	3±1
Exp. (Ref. 13)	9	530±26	1.05±0.05	9±1
QCT	9		0.73±0.06	8±1
Exp. (Ref. 13)	16	620±31	1.23±0.06	10±1
QCT	16		1.14±0.07	10±1

TABLE XII. Experimental and QCT rotational data for the $H+HCN(\nu_1,0,\nu_3,j=9)\rightarrow H_2+CN(v'=0,j')$ reaction, $E_T=0.83$ eV.

	HCN vib. state	$\langle E_{ROT}\rangle$	j'_{mp}	$\langle j'\rangle$
Exp. (Ref. 13)	002	1.08±0.05	9±1	13.6±0.7
QCT	002	0.80±0.07	6±1	8.72±0.52
Exp. (Ref. 12)	004	0.93±0.05	9±1	12.8±0.6
QCT	004	0.73±0.06	8±1	9.37±0.63
QCT	302	0.96±0.05	9±1	9.70±0.88

Boltzmann distributions. As an alternative, we have studied the evolution of the CN rotational excitation for different rotational states of the parent HCN. The resulting average rotational energy and most populated rotational levels are compared with the available experimental information in Table XI. Also, the QCT CN($v'=0$) rotational populations for the different rotational states of HCN studied have been compared with the experimental Maxwell–Boltzmann fits in Fig. 6.

Although the CN rotational distributions of the $H+HCN(002,j=9)$ reaction were also measured with $E_T=0.83$ eV, no experimental characterization of CN rotation for the reaction with HCN(302) at this translational energy is available. Table XII collects the available experimental data on CN($v'=0$) rotation for the $H+HCN(002,j=9)$ and $H+HCN(004,j=9)$ reactions for an E_T of 0.83 eV along with QCT results for these two HCN states and for the results of the experimentally unresolved $HCN(302,j=9)$ data.

The QCT results show that although the CN($v'=0$) product is slightly rotationally colder than the experimental data, the agreement with the experiment is rather good if uncertainties are included. Furthermore, analysis of the CN average rotational energy suggests that CN rotation is not affected by HCN vibrational excitation. This contrasts with the strong dependence of CN rotation on HCN rotational excitation that is evident from the results. This dependence follows logically from simple kinematics: the abstraction of the H atom from HCN during reaction has little effect on the rotational angular momentum of the CN that remains.

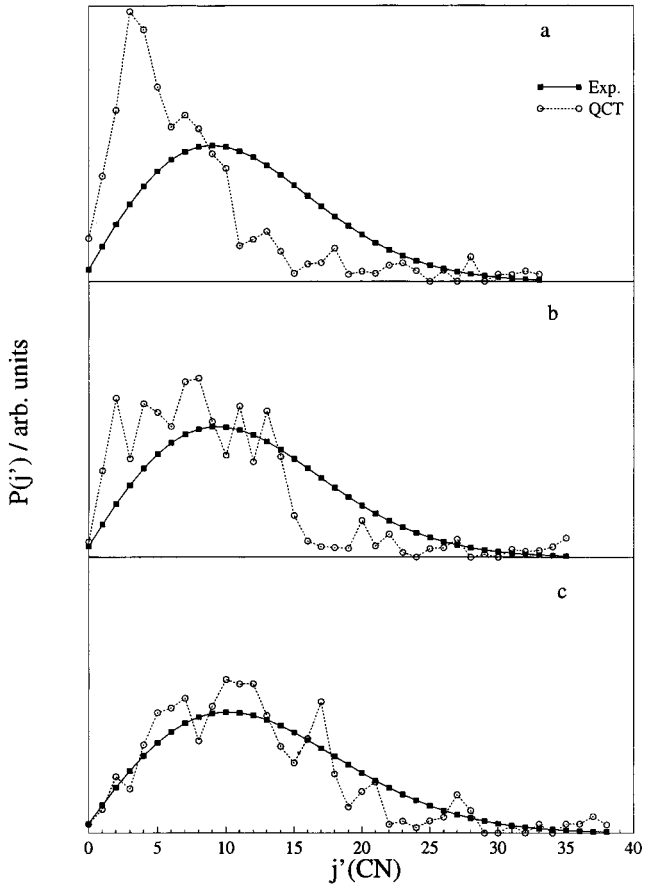

FIG. 6. Experimental and QCT CN($v'=0$) rotational distributions for the $H+HCN(004,j)\rightarrow H_2+CN(v'=0,j')$ reaction with $E_T=0.83$ eV, j(HCN) $=2$ (a), j(HCN)$=9$ (b) and j(HCN)$=16$ (c). All the distributions have been normalized to unity for the common j'(CN) values.

V. CONCLUSIONS

A quasiclassical trajectory study of the $H+HCN\rightarrow H_2+CN$ reaction dynamics has been performed. Not only the HCN ground vibrational state, but also a wide variety of excited vibrational states have been studied, comparing the results of the QCT dynamics with the experimental data where available. In general, there is quite good agreement between the results obtained here and experiment for all the initial HCN states considered and all the properties compared, suggesting that the potential energy surface used here is quite accurate in the regions that involve the H_2+CN products formation from the H+HCN reagents. Although H+HCN is primarily an abstraction reaction, the H_2CN minimum has a nonnegligible contribution to the reaction at high translational energy.

For the HCN ground state, we find rather good agreement between the experimental and QCT vibrational distributions at three different collisional energies. Vibrational excitation of the H_2 product has been reported, and this increases with reagent translational energy. CN vibrational excitation is much smaller, and the average vibrational energy increases slowly with reagent translational energy. The agreement with experiment is poorer with respect to rotational distributions, the experimental average rotational energies of CN being about twice the QCT ones. The angular distributions (referred to the CN molecule) show forward scattering at low E_T. At higher energy there is less forward scattering, as would be expected when stripping dynamics becomes important. However, H_2CN complex formation also plays a role at high energy. The parallel $\mathbf{j}'_{HH}\mathbf{j}'_{CN}$ angular distributions suggest that the product molecules have some ten-

dency to rotate in the same plane, which is the expected behavior for a reaction where planar geometries have the lowest energy.

When HCN vibrational excited states are considered, there is a good agreement not only between the QCT and experimental CN vibrational data but also in the rotational information, as occurs in the case of the HCN(002) state with $E_T = 0.83$ eV. The QCT and experimental CN rovibrational populations for the reaction with HCN(004) are also in good agreement for both thermal (300 K) translational energy and an energy of 0.83 eV. The vibrational enhancement of reactivity expected for a reaction with a late barrier, gives the (004) state a significant cross section for thermal conditions. Here we find that the dynamics is quite different from what is obtained at higher E_T. In particular, the reaction through the H_2CN minimum has a higher energy threshold than the direct one, so it does not contribute to the thermal energy cross section, playing a modest role at the experimental collisional energy. Also, both H_2 and CN are less rovibrationally excited than at higher E_T.

Although there is no experimental information available on the HCN(302) state, we have generated results for this state so that comparisons with other HCN states can be made. What we have learned from this study of HCN(302) is that there is strong enhancement in reactivity with respect to HCN(002), but not as much as for HCN(004). This suggests that the C–N mode is not as strongly coupled with motions leading to reaction as C–H stretch, however, the spectator model for the C–N stretch is far from describing its behavior satisfactorily.

ACKNOWLEDGMENTS

This research was supported by NSF Grant No. CHE-9873892 and by the Spanish Ministry of Education and Culture (M.E.C.) through the projects DGES PB98-1209-C02-01 and -02. D.T. thanks the M.E.C. for a Ph.D. Studentship and to Northwestern University for partial support.

[1] G. C. Schatz, M. ter Host, and T. Takayanagi, in *Computational Methods for Polyatomic Bimolecular Reactions*, edited by D. L. Thompson (World Scientific, Singapore, 1998).
[2] G. C. Schatz, Comput. Phys. Commun. **51**, 135 (1988).
[3] J. Huang, J. Valentini, and J. T. Muckerman, J. Chem. Phys. **102**, 5695 (1995).
[4] J. Berkowitz, G. B. Ellison, and D. Gutman, J. Phys. Chem. **98**, 2744 (1994).
[5] M. A. ter Horst, G. C. Schatz, and L. B. Harding, J. Chem. Phys. **105**, 558 (1996).
[6] G. A. Bethardy, A. F. Wagner, G. C. Schatz, and M. A. ter Horst, J. Chem. Phys. **106**, 6001 (1997).
[7] T. Carrington and S. V. Filseth, Chem. Phys. Lett. **145**, 466 (1988).
[8] H. M. Lambert, T. Carrington, S. V. Filseth, and C. M. Sadowski, J. Phys. Chem. **97**, 128 (1993).
[9] G. W. Johnston and R. Bersohn, J. Chem. Phys. **90**, 7096 (1989).
[10] R. A. Bair and T. H. Dunning, Jr., J. Chem. Phys. **82**, 2280 (1985).
[11] J. M. Pfeiffer, R. B. Metz, J. D. Thoemke, E. Woods III, and F. F. Crim, J. Chem. Phys. **104**, 4490 (1996).
[12] C. Kreher, R. Theinl, and K.-H. Gericke, J. Chem. Phys. **104**, 4481 (1996).
[13] C. Kreher, J. L. Rinnenthal, and K.-H. Gericke, J. Chem. Phys. **108**, 3154 (1998).
[14] K.-H. Gericke, C. Kreher, and E. A. Reinsch, J. Chem. Phys. **107**, 10567 (1997).
[15] D. C. Clary, J. Phys. Chem. **99**, 13664 (1995).
[16] A. N. Brooks and D. C. Clary, J. Chem. Phys. **92**, 4178 (1990).
[17] J.-H. Wang, K. Liu, G. C. Schatz, and M. ter Horst, J. Chem. Phys. **107**, 7869 (1997).
[18] K. S. Bradley and G. C. Schatz, J. Chem. Phys. **108**, 7994 (1998).
[19] R. D. Levine and R. B. Bernstein, *Molecular Reaction Dynamics and Chemical Reactivity* (Oxford University Press, New York, 1987).
[20] G. J. Germann, Y.-D. Huh, and J. J. Valentini, J. Chem. Phys. **96**, 1957 (1992).
[21] A. J. Orr-Ewing and R. N. Zare, Annu. Rev. Phys. Chem. **45**, 315 (1994).
[22] H. J. Loesch, Annu. Rev. Phys. Chem. **46**, 555 (1995).
[23] G.-S. Wu, G. C. Schatz, G. Lendvay, D.-C. Fang, and L. B. Harding, J. Chem. Phys. **113**, 3150 (2000).